Contrib Mineral Petrol (1984) 86:25–34

Contributions to Mineralogy and Petrology

Contrasting fluid/rock interaction between the Notch Peak granitic intrusion and argillites and limestones in western Utah: evidence from stable isotopes and phase assemblages

P.I. Nabelek [1], T.C. Labotka [2], J.R. O'Neil [3], and J.J. Papike [4]

[1] Department of Geology, University of Missouri, Columbia, Missouri 65211, USA
[2] Department of Geological Sciences, University of Tennessee, Knoxville, Tennessee 37916, USA
[3] Isotope Geology Branch, U.S. Geological Survey, 345 Middlefield Road, Menlo Park, California 94025, USA
[4] Institute for the Study of Mineral Deposits, South Dakota School of Mines and Technology, Rapid City, South Dakota 57701, USA

Abstract. The Jurassic Notch Peak granitic stock, western Utah, discordantly intrudes Cambrian interbedded pure limestones and calcareous argillites. Contact metamorphosed argillite and limestone samples, collected along traverses away from the intrusion, were analyzed for $\delta^{18}O$, $\delta^{13}C$, and δD. The $\delta^{13}C$ and $\delta^{18}O$ values for the limestones remain constant at about 0.5 (PDB) and 20 (SMOW), respectively, with increasing metamorphic grade. The whole rock $\delta^{18}O$ values of the argillites systematically decrease from 19 to as low as 8.1, and the $\delta^{13}C$ values of the carbonate fraction from 0.5 to -11.8. The change in $\delta^{13}C$ values can be explained by Rayleigh decarbonation during calc-silicate reactions, where calculated $\Delta^{13}C_{(CO_2\text{-}cc)}$ is about 4.5 permil for the high-grade samples and less for medium and low-grade samples suggesting a range in temperatures at which most decarbonation occurred. However, the amount of CO_2 released was not anough to decrease the whole rock $\delta^{18}O$ to the values observed in the argillites. The low $\delta^{18}O$ values close to the intrusion suggest interaction with magmatic water that had a $\delta^{18}O$ value of 8.5. The extreme lowering of $\delta^{13}C$ by fractional devolatilization and the lowering of $\delta^{18}O$ in argillites close to the intrusion indicates oxgen-equivalent fluid/rock ratios in excess of 1.0 and $X(CO_2)_F$ of the fluid less than 0.2. Mineral assemblages in conjunction with the isotopic data indicate a strong influence of water infiltration on the reaction relations in the argillites and separate fluid and thermal fronts moving thru the argillites. The different stable isotope relations in limestones and argillites attest to the importance of decarbonation in the enhancement of permeability. The flow of fluids was confined to the argillite beds (argillite aquifers) whereas the limestones prevented vertical fluid flow and convective cooling of the stock.

Introduction

One of the important aspects of contact metamorphism is the potential for mass exchange between an intrusion and country rocks. Driving forces for such exchange are pressure, temperature and chemical gradients, where important transport media are fluids of either magmatic or meteoric origin or those derived directly from devolatilization reactions in the country rocks. Much information about the temperature regime in a contact zone can be obtained from mineral assemblages and reaction relationships. In carbonate rich country rocks, such reactions are extremely sensitive to the H_2O/CO_2 ratio in coexisting fluids (Greenwood 1962). Rice and Ferry (1982) point-out, however, that mineral reactions can buffer fluid composition while infiltration occurs.

Numerous approaches have been used to determine the composition of metamorphic fluids. Hydrogen, carbon, and oxygen isotope ratios of whole rocks and mineral separates provide one of the most powerful tools, because they reflect the origin and isotopic composition of the fluids (e.g. Shieh and Taylor 1969a, b; Taylor 1974, 1977; Taylor and O'Neil 1977; Shelton 1983) and the relative amounts of dehydration, decarbonation, and infiltration (Rice 1977; Rumble 1982; Rumble et al. 1982; Tracy et al. 1983).

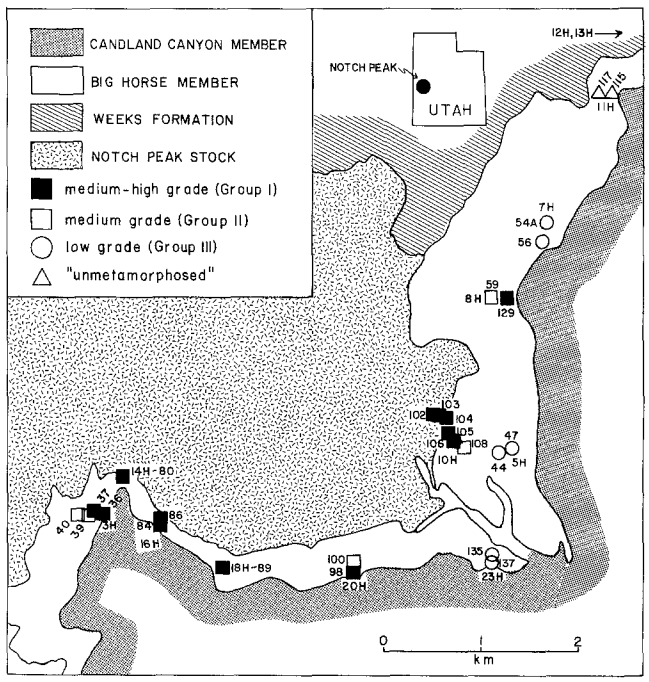

Fig. 1. Map of the Notch Peak metamorphic aureole with sample locations. The isograds are defined by mineral assemblages in the argillites listed in Table 2

Offprint requests to: P.I. Nabelek

Table 1. Chemical and isotopic analyses of Big Horse member samples

	Sample	Cycle	$\delta^{18}O$ (SMOW)	$\delta^{13}C$ (PDB)	δD (SMOW)	CaO wt.%[a]	CaO mole %[a]	CO_2 wt.%	CO_2 mole %
Argillites	11H-115	1	18.8	0.5	−78	41.1	38.5	32.4	38.6
	5H-47	1	18.0	−1.4	−81	33.7	34.5	22.8[a]	29.0
	23H-137	1	18.9	−3.2	−79	29.2	29.7	20.2	26.1
	7H-56	1	15.9	−1.7	−65	27.1	29.3	18.5	23.6
	8H-129	1	12.8	−10.0	−77	16.1	17.8	1.03	1.45
	20H-98	1	12.6	–	–	22.0	24.8	–	–
	18H-89	1	13.1	−2.6	−81	41.7	42.3	11.2	14.5
	16H-84	1	12.5	–	−78	29.2	33.7	–	–
	14H-80	1	12.6	–	−88	19.7	22.3	–	–
	3H-36	1	15.3	−5.7	–	16.9	19.4	0.57	0.83
	3H-37	1	10.5	−5.0	−73	32.2	35.2	2.64	3.63
	12H-123	2	18.8	1.4	−91	21.0	21.4	16.3	21.2
	11H-117	2	17.3	0.3	−75	16.7	17.3	13.0	17.0
	5H-44	2	17.3	−0.8	−78	21.9	24.0	6.97[a]	9.73
	23H-135	2	14.3	–	−65	9.9	10.9	–	–
	8H-59	2	11.9	−1.8	−59	17.5	19.4	2.30	3.39
	20H-100	2	10.7	–	−84	35.9	40.3	–	–
	16H-86	2	10.6	−9.3	−73	35.6	37.9	1.29	1.75
	3H-39	2	12.1	−3.1	−73	17.5	19.7	0.56	0.81
	3H-40	2	11.5	−6.5	−69	39.2	40.9	0.57	0.76
	10H-108	6	9.6	−2.5	−80	41.2	40.9	16.6	21.5
	10H-106	6	8.2	−5.8	−79	38.8	41.1	2.88	3.88
	10H-105	6	13.4	−2.6	−81	34.2	35.2	12.6	17.3
	10H-104	6	8.5	−10.0	−59	34.6	36.1	2.74	3.69
	10H-103	6	8.1	−11.8	−63	34.7	26.8	3.74	5.06
	10H-102	6	9.7	−7.3	−66	27.1	30.1	3.17	4.49
Limestones	12H-122	2	20.4	0.6	–	52.3	46.5	43.5[a]	49.3
	11H-116	2	20.4	0.7	–	52.6	46.8	43.7	49.0
	5H-46	2	20.3	0.4	–	51.3	44.8	42.6	47.4
	23H-136	2	20.3	0.6	–	52.8	47.0	43.6	49.5
	7H-55	2	20.3	0.4	–	52.8	47.2	45.0	49.2
	8H-130	2	20.1	1.0	–	52.5	47.6	43.0	48.7
	20H-99	2	20.6	0.8	–	51.2	45.5	42.9	48.6
	18H-90	2	20.5	0.4	–	52.0	46.4	42.7	48.6
	16H-85	2	20.6	0.5	–	51.4	45.8	43.1	48.9
	14H-81	2	20.4	0.5	–	49.1	43.6	41.5	46.9
	3H-38A	2	20.4	0.6	–	50.6	45.3	43.3	49.4
	11H-118	4	21.0	0.6	–	52.4	–	44.1	–
	23H-134	4	21.1	0.5	–	52.9	–	44.5	–
	8H-112	4	21.1	0.3	–	52.9	–	42.1[a]	–
	10H-111	4	20.7	0.3	–	50.5	–	42.8	–
	13H-126	5	20.3	0.7	–	53.0	–	43.3[a]	–
	11H-119	5	20.5	0.3	–	43.4	–	37.4	–
	8H-113	5	20.2	0.0	–	51.6	–	43.3[a]	–
	13H-127	6	20.4	−0.1	–	52.7	–	41.7[a]	–
	11H-121	6	18.5	−0.8	–	45.0	–	36.6	–
	8H-114	6	19.1	−1.1	–	53.0	–	40.0[a]	–
	10H-107	6	20.0	−0.4	–	49.4	–	40.2[a]	–

[a] From Hover (1981)

In this paper, we use stable isotope analyses of interbedded argillites and limestones of the Big Horse member of the Orr formation, Utah, to determine the paths and composition of the fluids in the country rocks during metamorphism and the relative importance of internal fluid buffering and infiltration of fluid from the crystallizing Notch Peak granitic stock. In conjunction with the work of Hover-Granath et al. (1983) on the mineralogy and petrology of the Big Horse member, the stable isotope data provide the opportunity to determine the temperature-$X(CO_2)_F$-time relations during infiltration and devolatilization and the relative effects of decarbonation in pure limestones and calcareous argillites on permeability.

Geology of the Big Horse member of the orr formation

The details of the geology of the Big Horse member of the Orr formation are described in Hover-Granath et al. (1983) and only a summary is given here.

The Upper Cambrian Big Horse member of the Orr formation was intruded by the 165 m.y. old (unpublished $^{40}Ar/^{39}Ar$ biotite data) Notch Peak granitic stock (Fig. 1) whose petrogenesis has been described by Nabelek et al. (1983, 1984a, b). The Big Horse member is a miogeoclinal sequence of six upward-shallowing cycles, each of which consists of a calcareous argillite toward the bottom and a pure limestone toward the top. The tectonically undis-

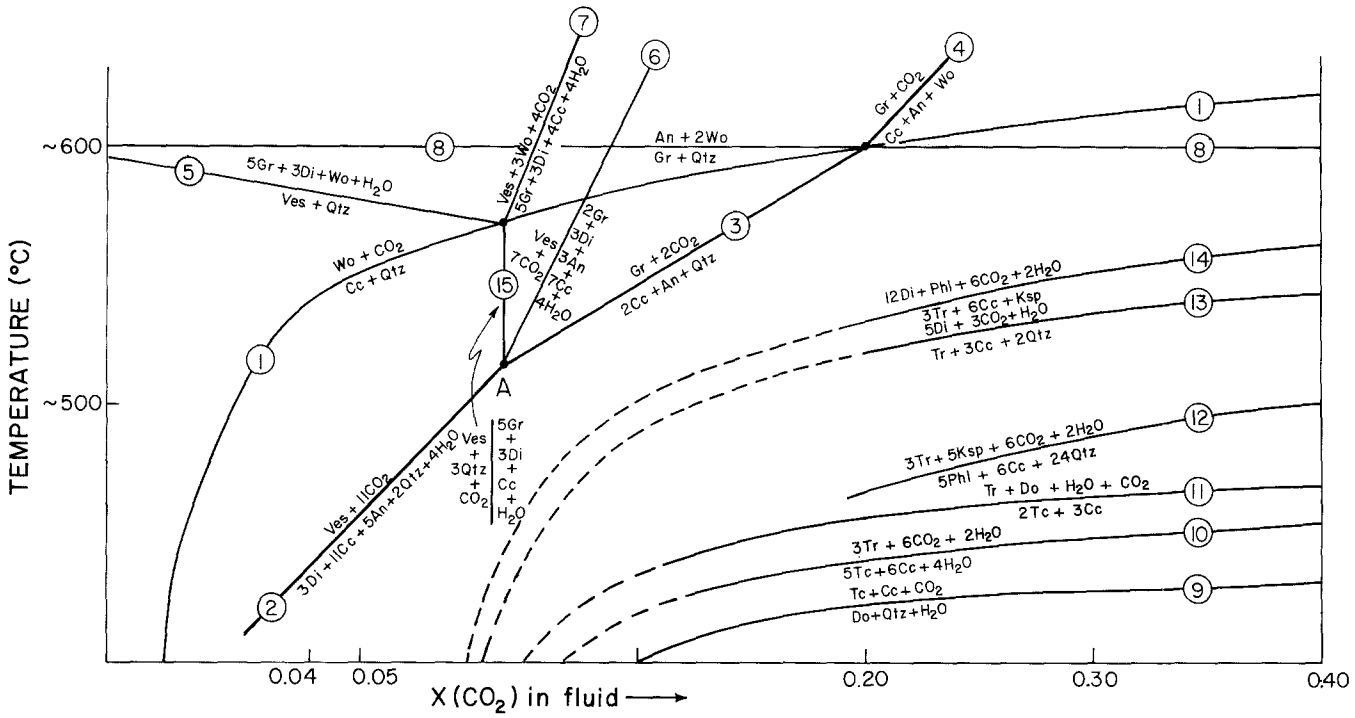

Fig. 2. Temperature – $X(CO_2)_F$ diagram applicable to the Notch Peak assemblages. Group I argillite samples (see text) are those that crossed garnet-producing reaction 3 or 4; Group II argillite samples are those that crossed vesuvianite-producing reaction 2. Low-grade argillite samples (Group III) have evidence for reactions 9–14 that occur to the CO_2-rich part of the diagram. These, and high-temperature forsterite-producing reactions (not shown) also occurred in the limestones (Hover-Granath et al. 1983). Note the expanded scale at the low $X(CO_2)_F$ part of the diagram

turbed cycles, which were discordantly cut by the stock, can be traced over a distance of several kilometers from the contact and thus provide an exceptional opportunity to describe a contact metamophic event. The sedimentary rocks were not metamorphosed prior to or after the stock's emplacement at a pressure of 1.5 kbar (Nabelek et al. 1984b). Samples from complete traverses of cycle 1 argillite, cycle 2 argillite and limestone, and few additional samples from other cycles were analyzed for stable isotope compositions (Table 1). The complete petrologic description of the samples is given in Hover-Granath et al. (1983) and the complete major-element whole rock and mineral analyses are given in Hover (1981).

Mineral assemblages

Although stable isotope data alone can provide information about fluid/rock ratios, fluid composition and temperatures, metamorphic reactions aid in deducing a temperature-$X(CO_2)_F$ path. Figure 2 is a T-$X(CO_2)_F$ diagram after Kerrick (1974) and Eggert and Kerrick (1981) that is applicable to reactions in the argillites. Assemblages in high to medium grade samples (10H-102, 103, 104, 105, 106, 14H-80, 16H-86, 84, 3H-37, 18H-89, 3H-36, 20H-98, and 8H-129) are consistent with garnet-producing reactions and reaction 7 to the CO_2-rich side of invariant point A, while assemblages in medium-grade samples (8H-59, 20H-100, 3H-39, 40, and 10H-108) are consistent with vesuvianite-producing reactions to the water-rich side of point A (Table 2). Although the temperature in the high-grade samples likely approached 600°, it is noted that quartz-consuming reactions 5 and 8 did not occur due to the silica-poor composition of the rocks as evidenced by the lack of quartz in most. All or most quartz was consumed by wollastonite-producing reaction 1.

We call the group of samples that falls to the CO_2-rich side of point A "Group I" and the group that falls to the H_2O-rich side "Group II". "Group III" consists of low-grade samples (Station 5H, 7H, and 23H) that have assemblages consistent with reactions 9–14 that occur in equilibrium with more CO_2-rich fluids. These and forsterite-producing reactions that occur at higher temperatures are also applicable to describe reaction relations in the limestones (Hover-Granath et al. 1983).

Analytical techniques

The whole rock samples from the Big Horse member were analyzed by conventional extraction techniques and isotope ratio mass spectrometry. All δ values (Table 1) are given in standard permil deviations relative to the SMOW standard for oxygen and hydrogen and to the PDB standard for carbon. Carbon and oxygen isotope compositions of the carbonates were determined on CO_2 that was liberated by 100% phosphoric acid (McCrea, 1950). Pure limestone samples containing only 2 to 4 wt.% MgO and 1–3 wt.% SiO_2 were reacted at 25° C, while the carbonate fractions of the argillites were reacted at 50° C. The reproducibility of replicate analyses is better than ± 0.1 permil for both $\delta^{13}C$ and $\delta^{18}O$ values.

Oxygen from whole rock argillite samples was liberated by reaction with BrF_5 in Ni bombs at 600° C (Clayton and Mayeda 1963). The oxygen was converted to CO_2 by reaction with a hot carbon rod.

Water was liberated from the argillites by induction heating and reacted with hot uranium metal to produce hydrogen for analysis (Bigeleisen et al. 1952). The reproducibility for the D/H analyses is better than ± 1.0 permil.

Results

The most important first-order observation of this study is that the contact metamorphic event affected the $\delta^{18}O$

Table 2. Mineral assemblages in Big Horse argillites[a]

	Quartz	Calcite	K-feld-spar	Plagio-clase	Mus-covite	Biotite	Trem-olite	Diop-side	Wol-lans-tonite	Gros-sular	Vesu-vianite	Scap-olite	Clays
Unmetamorphosed													
12H-123	×	×	×	×	×	×							×
11H-115	×	×		×	×	×							×
11H-117	×	×	×	×	×								×
Group 3													
5H-44	×	×	×	×		×		×				×	
5H-47	×	×	×				×	×					
23H-135	×	×	×	×		×	×	×					
23H-137	×	×	×	×		×	×						
7H-54A	×	×	×	×		×	×	×					
7H-56	×	×	×	×			×	×				×	
Group 2													
8H-59		×	×	×		(×)		×			×		
20H-100		(×)		×				×	×		×		
3H-39	×	×	×	×				×	×		×		
3H-40		×						×	×		×		
10H-108		×	×	×				×	×		×		
Group 1													
8H-129	×	×	×	×				×		×		×	
20H-98		(×)	×	×				×	×	×			
3H-36		(×)	×	×				×	×	×			
18H-89		×	×	×				×	×	×	×		
3H-37		(×)	×	×				×	×	×	×		
16H-86	(×)	(×)	×	×				×	×	×	×		
16H-84		×	×	×				×	×	×	×		
14H-80		(×)	×	×				×	×	×	×		
10H-106		×	×	×				×	×	×	×		
10H-105		×	×	×				×	×	×	×		
10H-104	×	×	×					×	×	×	×		
10H-103		×						×	×	×	×		
10H-102	×	×		×				×		×	×		

( ) Only trace amount of the phase present

[a] After Hover-Granath et al. (1983)

values of the limestones and the argillites very differently (Fig. 3). The samples are arranged according to grade as determined by the distance from the contact and mineral assemblages. The cycle 2 limestone contains a maximum of 3 wt.% SiO_2 and 5 wt.% MgO and thus consists essentially only of calcite. The $\delta^{18}O$ values of around 20 remained unchanged even though, as reported by Hover-Granath et al. (1983), the high grade samples lost all sedimentary structures and fossils. The $\delta^{13}C$ values also remained unchanged at around 0.5 (Table 1). These $\delta^{18}O$ and $\delta^{13}C$ values are typical for Cambrian limestones (Hoefs 1973). The isotopic composition of the clean limestone beds was clearly unaffected by the contact metamorphism.

The $\delta^{18}O$ values of cycle 1 and 2 argillites systematically decrease with metamorphic grade from about 19 to about 11 while in cycle 6 at station 10H to values as low as 8.1 (Table 1; Fig. 3). Concomitant with the change in $\delta^{18}O$ is a decrease in $\delta^{13}C$ values of the carbonate minerals in the argillites from 0.5 in the unmetamorphosed samples to −11.8 near the contact (Fig. 4). The difference in the variation of the oxygen and carbon isotope ratios between the argillites and limestones is striking; the contact metamorphism has left a much stronger imprint on the isotopic composition of the argillites than on the limestones.

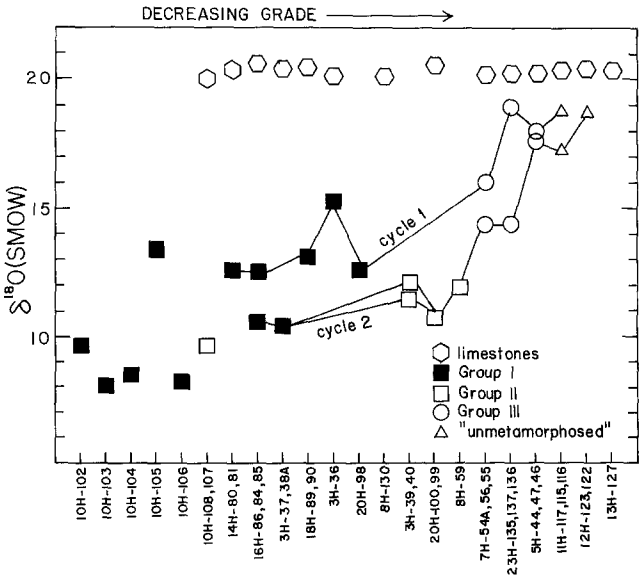

Fig. 3. Plot of $\delta^{18}O$ against metamorphic grade for Big Horse limestones and argillites. Note the constant $\delta^{18}O$ values of the limestones and the systematically decreasing $\delta^{18}O$ values of the argillites with metamorphic grade

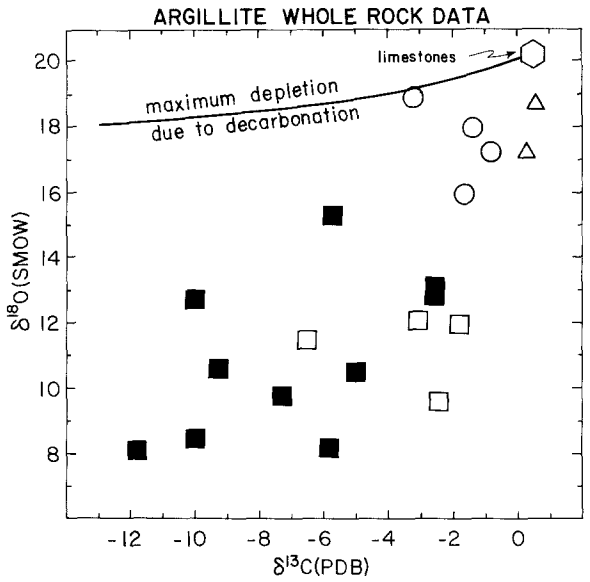

Fig. 4. Plot of $\delta^{18}O$ against $\delta^{13}C$ in the argillites. Note the systematic decrease of $\delta^{13}C$ with $\delta^{18}O$. Also shown is the path for maximum lowering of δ-values due only to decarbonation

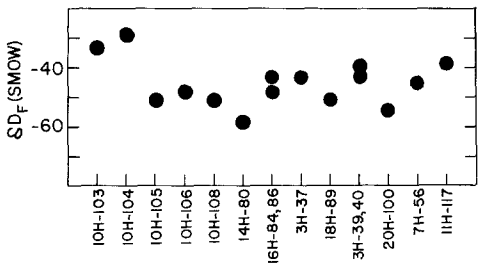

Fig. 5. Plot of calculated δD values of a fluid that would have been in equilibrium with hydrous phases in the argillites. These values are inconsistent with D values of local meteoric water but are the same as that of a magmatic fluid that would have exsolved from the crystallizing stock. The samples are in the same order of decreasing metamorphic grade as in Fig. 2

Hydrogen isotope analyses of the argillites are given in Table 1. Most δD values fall between -80 and -65. For those samples that contain 2 or more hydrous phases, the δD values are only of qualitative use. More information can be obtained from those samples that contain only one hydrous phase, in this case vesuvianite or tremolite.

Calculated δD values of a fluid that may have been in equilibrium with samples containing only vesuvianite or tremolite are shown in Fig. 5. The δD values were calculated using the fluid-mineral fractionation equation of Suzuoki and Epstein (1976), where appropriate mineral compositions were taken from Hover (1981). It was assumed that the equation is also applicable to fluid-vesuvianite fractionation, although Suzuoki and Epstein did not conduct experiments involving vesuvianite. A temperature of 600° C was assumed for sample 3H, 14H, and 16H, 525° C for 18H, 20H, and 8H, 400° C for 23H, and 300° C for 11H. These temperatures are based on the application of calcite-dolomite geothermometry to the adjacent cycle 2 limestone (Hover-Granath et al. 1983). Results indicate that the δD value of a water-rich fluid in equilibrium with the samples must have been about -50. This value is the range of primary magmatic water values (Taylor 1974).

In summary, the contact metamorphism had a strong effect on the isotopic composition of the argillites and very little effect on the isotopic composition of the limestones. Therefore, most of the following discussion deals with the relations between time, temperature and fluid composition in the argillites. The explanation and implications of the different isotopic compositions of the two rock types will be discussed after presentation of the calculations.

Fluid interaction between the intrusive and argillites

Decarbonation

Increasing temperature causes decarbonation reactions to proceed in calc-silicate rocks. Because $\Delta^{13}C_{(CO_2\text{-calcite})}$* becomes positive at $T > 200°$ C (Bottinga 1968), decarbonation reactions lead to a decrease in $\delta^{13}C$ values of the remaining calcite. A Rayleigh distillation process is especially effective in lowering $\delta^{13}C$ values of calcite undergoing decarbonation and the changes in $\delta^{13}C$ values reflect the temperature dependent fractionation factor and the amount of decarbonation (e.g. Lattanzi et al. 1980; Rumble 1982). If both the original and final $\delta^{13}C$ values of calcite and the amount of CO_2 lost from the rock are known, it is possible to calculate the time-integrated average α value during decarbonation of each sample:

$$\alpha = \frac{\ln\left[\frac{1000+\delta^{13}C^{f}}{1000+\delta^{13}C^{i}}\right]}{\ln F} + 1$$

where $\delta^{13}C^{i}$ is the initial value (0.5) and $\delta^{13}C^{f}$ is the measured value. The fraction of CO_2 lost (F) can be determined from the known amounts of CO_2 and CaO in each sample because calcite was originally essentially the only mineral that contained calcium.

The calculated $\Delta^{13}C$ values are tabulated in Table 3 and plotted against metamorphic grade in Fig. 6. The calculations indicate that the integrated $\Delta^{13}C_{(CO_2\text{-CC})}$ values during decarbonation of the highest-grade samples was about 4.5 permil, while the *apparent* $\Delta^{13}C$ values for lower-grade samples are as small as 1.1. The smaller $\Delta^{13}C$ values indicate either: 1) approach toward batch (as opposed to Rayleigh) decarbonation with $\Delta^{13}C$ of 4.5, or 2) Rayleigh decarbonation with lower $\Delta^{13}C$ and thus lower temperature. For most samples it is difficult to distinguish between the two choices but as shown in Fig. 7, the $\Delta^{13}C$ value during decarbonation of most Group II samples must have been less than 4.5 and therefore decarbonation occurred at a lower temperature.

The apparent $\Delta^{13}C$ values of most low-grade samples are unrealistically large and they are ascribed to the presence of scapolite where the carbon in CO_2 that is likely present in the mineral may be unusually isotopically light. The presence of scapolite may also explain the rather large calculated $\Delta^{13}C$ value for sample 8H-129 which is too high for the grade of the sample (Fig. 6). Therefore, this sample will be ignored in further discussions. Carbon isotopic fractionation factors between CO_2 and scapolite are not known and therefore it is difficult to evaluate if this is a viable explanation.

* $\Delta^{13}C_{(CO_2\text{-CC})} = 10^3 \ln \alpha\,(CO_2\text{-CC})$ where $\alpha(CO_2\text{-CC}) = \frac{^{13}C/^{12}C(CO_2)}{^{13}C/^{12}C(CC)}$

Table 3. Calculated values of the amount of decarbonation, $\Delta^{13}C_{(CO_2\text{-}cc)}$, fluid/rock ratios, and fluid composition

Sample	Group	F_{CO_2} left	$\Delta^{13}C_{(CO_2\text{-}cc)}$	% rock lost as CO_2		$\delta(^{18}O)^f_R - \delta(^{18}O)^i_R$	Open system oxygen-equivalent H_2O/rock	V_{CO_2} lost/ V_{rock}	Maximum $X(CO_2)_F$
				wt.%	mole%				
10H-102	1	0.15	4.1	18.1	25.6	−8.9	1.3	0.8	0.16
10H-103	1	0.14	6.2	23.5	31.8	−10.0	2.0	1.1	0.14
10H-104	1	0.10	4.6	24.2	32.5	−9.8	1.8	1.1	0.16
10H-105	1	0.49	4.4	13.6	17.8	−6.2	0.6	0.6	0.21
10H-106	1	0.09	2.7	27.6	37.2	−10.6	2.0	1.3	0.16
10H-108	2	0.53	4.2	15.4	19.4	−9.9	1.4	0.7	0.11
16H-86	1	0.05	3.2	26.8	36.2	−7.8	1.1	1.3	0.25
3H-37	1	0.10	2.4	23.0	31.6	−8.4	1.1	1.1	0.22
18H-89	1	0.34	2.9	21.5	27.8	−6.3	0.7	1.0	0.29
3H-36	1	0.04	1.9	12.7	18.5	−3.5	0.3	0.6	0.36
8H-129	1	0.08	4.2[a]	11.7	16.4	−5.5	0.6	0.5	0.21
3H-39	2	0.04	1.1	13.1	18.9	−7.1	0.8	0.6	0.19
3H-40	2	0.02	1.8	30.2	40.1	−7.2	0.9	1.4	0.31
8H-59	2	0.18	1.3	11.3	16.0	−16.0	0.9	0.5	0.15
7H-56	3	0.80	9.8[a]	4.6	5.9	−3.8	0.3	0.2	0.16
23H-137	3	0.88	29.2[a]	2.8	3.6	−0.2	0.02	0.1	0.64
5H-44	3	0.41	1.4	10.2	14.2	−1.6	0.2	0.5	0.40
5H-47	3	0.84	10.9[a]	4.3	5.5	−2.5	0.1	0.2	0.30

[a] These values may be due to the presence of scapolite

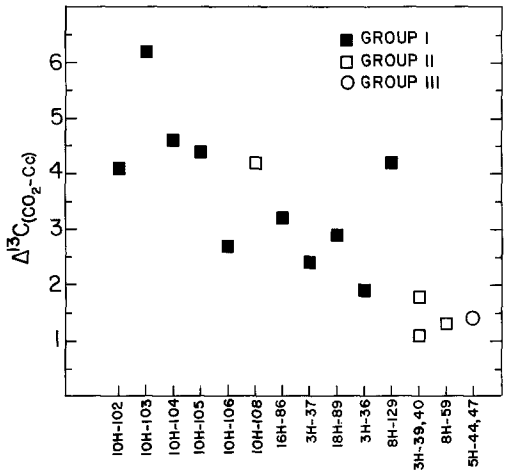

Fig. 6. Plot of calculated $\Delta^{13}C_{(CO_2\text{-}cc)}$ values against metamorphic grade. Note the systematic increase of the $\Delta^{13}C_{(CO_2\text{-}cc)}$ values with metamorphic grade, except for sample 8H-129 and low-grade samples 5H-47, 7H-56, and 23H-135, 137 (not shown) which yield unrealistically large values, probably due to the presence of scapolite

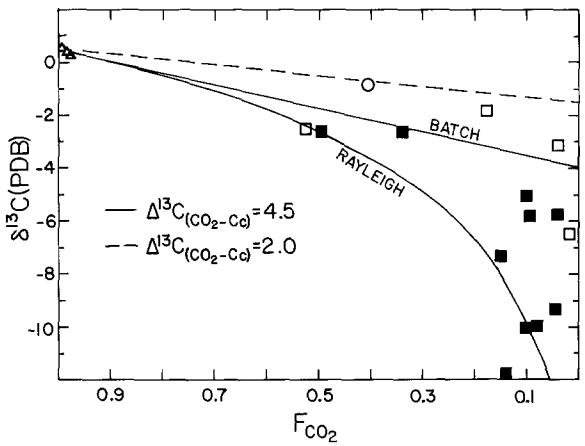

Fig. 7. Plot of measured $\delta^{13}C$ values against fraction of CO_2 left in the argillites. Also shown are theoretical paths of $\delta^{13}C$ decrease for Rayleigh and batch decarbonation using a $\Delta^{13}C_{(CO_2\text{-}cc)}$ value of 4.5 and batch decarbonation using a $\Delta^{13}C_{(CO_2\text{-}cc)}$ value of 2.5

Nevertheless, the $\Delta^{13}C$ value of 4.5 obtained for the high-grade samples may seem too large in light of Bottinga's (1968) calculations that show a maximum fractionation factor of about 3 permil at about 400° C. Although kinetic disequilibrium during decarbonation may explain the 6.2 permil fractionation factor for sample 10H-103 and the 4.5 permil factor, the 4.5 value may represent an equilibrium fractionation factor for 500–600° C range because:

1) If a fractionation of 3 permil is assumed for the high-grade samples, calculations would require an extreme CO_2 loss. If the calculated amount of CO_2 is then put back into the whole rock analyses, the amount of CO_2 exceeds the amount of calcium + magnesium to make calcite + dolomite.

2) The carbon isotope fractionation between calcite and graphite at 600° C (Bottinga, 1968) would agree better with the field-calibrated calcite-graphite geothermometer of Valley and O'Neil (1981) if the CO_2-calcite fractionation 600° C was 5 instead of 3. This is supported by the recent work of Wada and Suzuki (1983), but the work of Kreulen and van Beek (1983) agrees more with Bottinga (1969).

Therefore, there are two lines of evidence suggesting that the calculated CO_2-calcite fractionation factors of Bottinga (1968) may not be appropriate for use above 400° C.

Our calculations indicate that in samples closest to the contact with the intrusion, most decarbonation between 500° and 600° C was Rayleigh, while at lower grades most decarbonation occurred at lower temperatures and may not have been completely fractional (Figs. 6, 7).

Infiltration

Given the amount of decarbonation in the argillites (Table 3), it is possible to estimate the effect of decarbonation on the whole rock $\delta^{18}O$ values. Because of incomplete information about the temperature and the percentage of Rayleigh decarbonation for each sample, a limiting example may be decarbonation of the most calcium rich high-grade argillites 10H-102, 103, 104, 106, 16H-86, 3H-40, 18H-89 assuming $\Delta^{18}O_{(CO_2\text{-calcite})}$ of 8 permil (Bottinga 1968). The maximum calculated $\delta^{18}O$ *vs.* $\delta^{13}C$ depletion path for these samples is shown in Fig. 4. Clearly, the $\delta^{18}O$ values cannot be lowered to those observed in the metamorphosed argillites by decarbonation alone. This is because CO_2 accounts for only a small fraction of oxygen in the rock. The small amount of dehydration would tend to increase the $\delta^{18}O$ values because of negative water-mineral oxygen isotope fractionations below 500° C (Friedman and O'Neil 1978). Therefore, another mechanism must be invoked to explain the observed ^{18}O depletion.

Exchange with an infiltrating fluid of relatively low $\delta^{18}O$ value most easily explains the ^{18}O depletion. Infiltration has been proposed by others to explain similar isotopic data (e.g. Rumble et al. 1982; Tracy et al. 1983; Shelton 1983), and element transport (Ferry 1978, 1982, 1983). Meteoric water can be ruled out as the low ^{18}O source, because a) the oxygen isotope compositions of the limestones are not compatible with a vertical movement of a low ^{18}O fluid and b) the δD values of the argillites (Table 1; Fig. 5) are too high for interaction with meteoric fluids to have taken place. Furthermore, there is no evidence for interaction of the stock with low D meteoric fluids (Nabelek et al. 1983). The most obvious fluid reservoir that is relatively depleted in ^{18}O is fluid that exsolved from the crystallizing stock.

Due to the small oxygen isotope fractionation factors between feldspars and water at magmatic temperatures (O'Neil and Taylor 1967) it can be safely assumed that a water-rich magmatic fluid exsolving from the crystallizing stock had a $\delta^{18}O$ value near 8.5, the average value of feldspars in the stock (Nabelek et al. 1983). Oxygen isotope exchange between the argillites and the infiltrating magmatic fluid can explain the lowering of $\delta^{18}O$ values in the argillites. The amount of ^{18}O depletion in excess of that possible by devolatilization (Table 3) can be used to estimate water/rock ratios.

Fluid/rock ratios and fluid composition

The volume of CO_2 generated by decarbonation can be directly estimated from the amount of CO_2 lost from each sample (Table 3). It was assumed that the specific volume of CO_2 is 1.72 cm^3g^{-1} at 610° and 1,500 bar (Shmonov and Shmulovich 1974) and the specific volume of rock is 0.37 cm^3g^{-1}. As shown in Table 3, the total volume of CO_2 produced on decarbonation was 0.5 to 1.3 times the volume of rock. The consequent build-up of pressure must have increased pore space and permeability of the rock.

Taylor (1977) formulated an equation that describes stable isotope exchange between an infiltrating fluid and the host rock in an open system:

$$F/R = \ln\left[\frac{\delta_F^i - \Delta - \delta_R^i}{\delta_F^i - \delta_R^f - \Delta}\right]$$

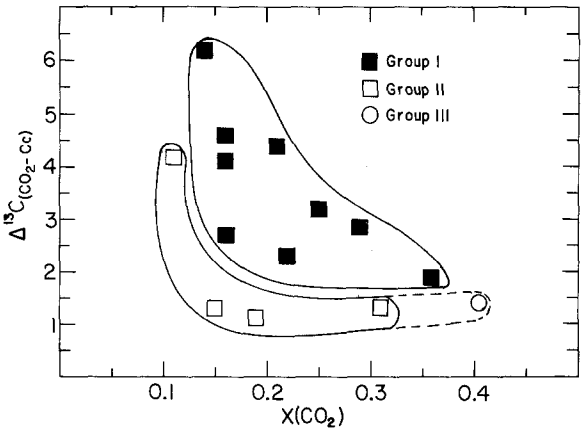

Fig. 8. Plot of calculated $\Delta^{13}C_{(CO_2\text{-cc})}$ values for the argillites against the maximum CO_2 content of the fluid in equilibrium with the rocks. Note that the position of Groups I, II, and III mirrors the reactions that occured in these samples in $T-X(CO_2)_F$ space

where δ_F^i and δ_R^i are the initial δ values of the fluid and rock, respectively, δ_R^f is the final δ value of the rock, and $\Delta = \delta_F^f - \delta_R^f$, where δ_F^f is the final δ value of a fluid increment. Under the assumption that during metamorphism of the argillites the infiltrating fluid made only one pass, the water/rock ratio can be estimated.

The $\delta_R^i(^{18}O)$ values equal to those along the $\delta^{18}O$ *vs.* $\delta^{13}C$ depletion path due to decarbonation (Fig. 4) and $\delta_F^i(^{18}O)$ values equal of 8.5 (magmatic fluid) were used. Although we don't have an estimate of modal mineralogy, most of the high-grade argillites are composed of garnet, diopside, wollastonite, and vesuvianite (Table 2) and therefore $\Delta^{18}O_{(H_2O\text{-rock})}$ value of 2.0 permil is probably safe to assume for a temperature of 500° to 600° C (Friedman and O'Neil 1977). Furthermore, fluid inclusions in the garnet and vesuvianite grains suggest that the fluid was rather saline (Feldman and Papike 1981), where the dissolved chlorine would have a tendency to increase the $\Delta^{18}O_{(H_2O\text{-rock})}$ value above 0 (Truesdell 1974). It is noted, however, that the recent laboratory study of Kendall et al. (1983) disputes Truesdell's work. The results (Table 3) suggest oxygen-equivalent water/rock ratios in excess of 1 for most samples. The water/rock values are minimum because it is unlikely that each increment of the infiltrating water reacted with the argillites. An oxygen-equivalent F/R of 1 corresponds to a volume F/R of about 2.4, assuming that the specific volume of water is 1.97 cm^3g^{-1} at 600° C and 1,500 bar (Burnham et al. 1969).

The calculated water/rock ratios and the amount of CO_2 released yield maximum CO_2 contents in the fluid any time in contact with the argillites. The results (Table 3) show that the fluid must have had a very low CO_2 content, consistent with the phase assemblages (Table 2, Fig. 2). The calculated CO_2 contents are plotted against the calculated $\Delta^{13}C_{(CO_2\text{-cc})}$ (Fig. 8) indicating that the fluid in equilibrium with higher-grade rocks was more H_2O-rich than that in equilibrium with lower-grade samples. This correlation and the fact that the data for Group II samples fall below those of Group I samples requires further discussion.

Correlation with phase assemblages

The position of the three groups of samples on the $\Delta^{13}C_{(CO_2\text{-cc})} - X(CO_2)_F$ diagram (Fig. 8) mirrors the position

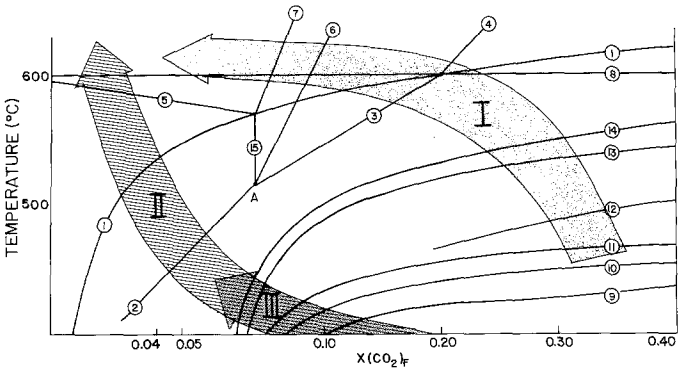

Fig. 9. Schematic diagram of $T-X(CO_2)_F$ paths of the three groups of rocks as determined from stable isotope data and mineral assemblages. High-grade rocks (Group I) followed a path of a temperature increase with subsequent H_2O infiltration. Medium-grade rocks followed a path of large amount of H_2O infiltration with a subsequent possible temperature increase (e.g. sample 10H-108) and low-grade rocks (Group III) represent merely an incomplete Group II path

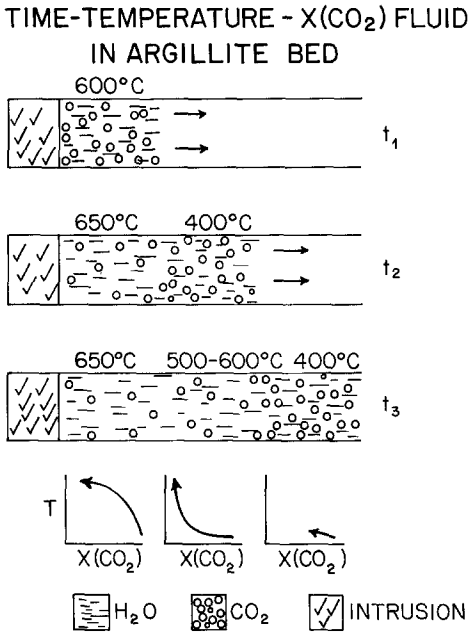

Fig. 10. Schematic diagram of fluid flow and temperature path with time (t_1, t_2, t_3) during contact metamorphism in a Big Horse member argillite bed (aquifer). The $T-X(CO_2)_F$ paths for high-, medium-, and low-grade samples are shown at the bottom of each figure and are the same as in Fig. 9. See text for discussion of this figure

of reactions that occured in these rocks in $T-X(CO_2)_F$ space (Fig. 2). The relatively larger $\Delta^{13}C_{(CO_2\text{-}cc)}$ fractionations and the larger apparent CO_2 contents in Group I, which comprises samples closest to the intrusive, suggest a rapid increase in temperature above 500° C in a relatively CO_2-rich fluid environment, followed by more H_2O infiltration with little further increase in temperature, such that reaction 7 occurred in most high-grade samples (Fig. 9).

Group II, consisting mostly of medium-grade samples, on the other hand, followed a path of relatively rapid H_2O infiltration by fluids emanating from the crystallizing magma, resulting in decarbonation reactions at about 400° C, followed by a temperature increase (Fig. 9). This path is suggested by a maximum $X(CO_2)_F$ of 0.2, lower $\Delta^{13}C_{(CO_2\text{-}cc)}$ values that suggest lower decarbonation temperature, and the evidence for reactions 1 and 2.

Lastly, the low-grade samples (Group III) have evidence for reactions that occur in a more CO_2-rich environment (Fig. 2). The larger $X(CO_2)_F$ values suggested by these reactions are consistent with calculated $X(CO_2)_F = 0.4$ for sample 5H-44 which lacks scapolite. We note that these samples did not have to reach temperatures much above 400 to 450° C, because the reactions shown can be crossed essentially isothermally if the fluids become progressively H_2O-rich due to water infiltration (Fig. 9). This path is consistent with the low $\Delta^{13}C_{(CO_2\text{-}cc)}$ value of 1.5 for sample 5H-44.

Discussion

The $T-X(CO_2)_F$ paths presented in Fig. 9 provide a description of fluid flow during contact metamorphism of calcareous argillites (Fig. 10). The results suggest that when the Notch Peak magma was emplaced (t_1; Fig. 10), there was a rapid temperature increase near the contact as expected from cooling models of Carslaw and Jaeger (1959). The rapid temperature increase to about 600° C caused relatively high-temperature decarbonation reactions to occur and the enhanced permeability allowed influx of H_2O, exsolved from the crystallizing magma (t_2). The high H_2O/CO_2 ratios and water/rock ratios suggested by phase assemblages and stable isotope data for the high-grade argillites are consistent with Rayleigh decarbonation where CO_2 was immediately removed by the infiltrating water. Rayleigh decarbonation is the only reasonable way to explain the low $\delta^{13}C$ values (Fig. 4). Although such low $\delta^{13}C$ values were explained by other authors by influx of ^{13}C-depleted fluid emanating from crystallizing intrusions (e.g. Taylor and O'Neil 1977; Kolodny and Gross 1974), such an interpretation is unlikely at Notch Peak because the large volume of CO_2 produced by the decarbonation reactions would overwhelm any CO_2 from the stock and because the suggested high H_2O/CO_2 ratios are inconsistent with CO_2 influx from the stock.

This model is in accord with that of Delaney (1982) who suggested (based on numerical solutions of pressurized fluid flow and temperature diffusion through sedimentary rocks) that on intrusion of a hot magma, there is a large gradient in fluid pressure in response to a sharp temperature difference between the rocks at the contact and sedimentary rocks further away from the contact. Therefore, an exsolving fluid will flow down the pressure gradient toward colder rocks. Delaney's numerical solutions further indicate that pore pressures in a rock where vapor, such as CO_2, is internally generated diffuse more rapidly than heat. This is in accord with the observations that in medium-grade samples the fluids became very H_2O-rich (t_2) prior to temperature increase above 500° C (t_3). The assemblages in the low-grade argillites resulted in response to the moving fluid front with a relatively larger CO_2 content and at lower temperatures at t_3. Thus, the present study clearly shows that internal decarbonation plays an important role in providing a mechanism for fluid infiltration from an external source and is in accord with Rumble et al. (1982) who suggested a similar correlation between decarbonation and infiltration.

This point is best exemplified by the lack of isotopic (Fig. 3) and mineralogic (Hover-Granath et al. 1983) evi-

dence for fluid flow through the pure limestones. Although the limestones were heated to temperatures in excess of 500° C, there is lack of isotopic evidence for extensive decarbonation (Table 1; Fig. 1). This is not surprising, because there were not enough silicate minerals to react with the calcite (±dolomite). The evident recrystallization of the limestones nevertheless indicates that there must have been some pore space in which the small amount of internally produced fluids resided. Therefore, comparing the argillites and limestones, it is evident that decarbonation reactions were necessary to enhance permeabilities to allow fluid flow through the Big Horse lithologies.

The lack of fluid flow through the limestones may have had an important effect on retarding fluid convection through the Notch Peak complex. Convection could have resulted in introduction of meteoric waters. However, there is no isotopic evidence in the wall rocks (this study) or the stock (Nabelek et al. 1983) for any interaction with meteoric waters. It is therefore suggested that the horizontal, undisturbed limestone beds blocked any vertical fluid flow, such that the flow was confined to horizontal movement in the argillites. This means that the intrusion must have cooled primarily by conduction of heat into the country rocks without significant contribution of convective cooling. The heat capacity of a water-rich fluid and the amount of fluid relative to the magma were too small for the fluid flow to significantly contribute to the cooling of the pluton. This is again supported by the $T-X(CO_2)_F$ paths of most of the argillite samples (Fig. 9) which primarily indicate a large influx of water followed by a temperature increase.

The different responses of the argillites and limestones to contact metamorphism shed light on the role of infiltration in the buffering of devolatilization reactions. The $T-X(CO_2)_F$ paths of the metamorphosed argillites (Fig. 9, 10) clearly indicate the crossing of reaction curves due to infiltration of H_2O from the intrusion yet the mineralogical evidence suggests completion of each reaction crossed (Hover-Granath et al. 1983). This indicates that the molecular constituency of fluid occupying pore space within the argillites at any one instant was controlled by an interplay between infiltration and mineral reactions. This is in accord with the work of Rice and Ferry (1982).

The stable isotope compositions of the limestones and mineral assemblages are, on the other hand, consistent with buffering of fluid composition by decarbonation reactions, (This study; Hover-Granath et al. 1983). Because more CO_2 than H_2O is produced during these reactions (Fig. 2), the fluids became progressively CO_2-rich to values of $X(CO_2)_F$ as high as about 0.8. The amount of fluids produced during these reactions was clearly too small to result in significant increase of permeability in the limestones and thus infiltration of magmatic fluid. Therefore, an important result of this study is that due to the much larger permeability of the argillites than the limestones, the argillites acted as metamorphic aquifers for the infiltrating magmatic fluid.

Acknowledgements. This research was funded by the D.O.E. grant DE-AC01-82ER-12050 (J.J. Papike) and by the U.S. Geological Survey. The authors thank G.N. Hanson for fruitful discussions. J. Ferry, F. Spear, and K. Shelton are thanked for critical review of the manuscript. Vicky Hover-Granath collected the samples and D. White and J. Drotleff assisted in the laboratory. Lori Frye is thanked for typing the manuscript. Figure preparation was funded in part by the University of Missouri Geology Development Fund. Part of the study was conducted during first, second and fourth authors' stay at SUNY-Stony Brook.

References

Bigeleisen J, Perlman JL, Prosser HC (1952) Conversion of hydrogenic materials to hydrogen for isotopic analysis. Anal Chem 24:1356

Bottinga Y (1968) Calculation of fractionation factors for carbon and oxygen exchange in the system calcite-carbon dioxide-water. J Phys Chem 72:800–808

Burnham CW, Holloway JR, Davis NF (1969) Thermodynamic properties of water to 1000° C and 10,000 bars. Geol Soc Am Spec Pap 132:96

Clayton RN, Mayeda TK (1963) The use of bromine pentafluoride in the extraction of oxygen from oxides and silicates for isotopic analyses. Geochim Cosmochim Acta 27:43–53

Carslaw HS, Jaeger JC (1959) Conduction of Heat in Solids, pp 510, Oxford Univ Press, New York

Delaney PT (1982) Rapid intrusion of magma into wet rock: Groundwater flow due to pore pressure increases. J Geophys Res 87:7739–7756

Eggert RG, Kerrick DM (1981) Metamorphic equilibria in the siliceous dolomite system: 6 kb experimental data and geologic implications. Geochim Cosmochim Acta 45:1039–1049

Ferry JM (1978) Fluid interaction between granite and sediment during metamorphism, south-central Maine. Am J Sci 278:1025–1056

Ferry JM (1982) A comparative geochemical study of pelitic shists and metamorphosed carbonate rocks from south-central Maine, USA. Mineral Petrol 80:59–72

Ferry JM (1983) Mineral reactions and element migration during metamorphism of calcareous sediments from the Vassalboro Formation, south-central Maine. Am Mineral 68:334–354

Feldman MD, Papike JJ (1981) Metamorphic fluid composition from the Notch Peak aureole, Utah. Abstract, EOS, Trans Am Geophys Union 62:435

Friedman I, O'Neil JR (1978) Hydrogen. In: Wedepohl KH (ed) Handbook of Geochemistry, 1. B-F, I, L. Springer-Verlag, New York

Greenwood HJ (1962) Metamorphic reactions involving two volatile components. Carnegie Inst Wash Yearb 61:82–85

Hoefs J (1973) Stable Isotope Geochemistry, Springer, New York

Hover VC (1981) The Notch Peak metamorphic aureole, Utah: Mineralogy, petrology, and geochemistry of the Big Horse Canyon Member of the Orr Formation. M.S. thesis, State Univ. New York, Stony Brook

Hover-Granath VC, Papike JJ, Labotka TC (1983) The Notch Peak contact metamorphic aureole, Utah: Petrology of the Big Horse limestone member of the Orr Formation. Geol Soc Am Bull 94:889–906

Kendall C, Chou I-M, Coplen TB (1983) Salt effect on oxygen isotope equilibria, Abstract, EOS, Trans Am Geophys Union 64:334

Kerrick DM (1974) Review of metamorphic mixed volatile (H_2O/CO_2) equilibria. Am Mineral 59:729–769

Kolodny Y, Gross S (1974) Thermal metamorphism by combustion of organic matter: isotopic and petrologic evidence. J Geol 82:489–506

Kreulen R, van Beek PCJM (1983) The calcite-graphite isotope thermometer; data on graphite bearing marbles from Naxos, Greece. Geochim Cosmochim Acta 47:1527–1530

Lattanzi P, Rye D, Rice JM (1980) Behavior of ^{13}C and ^{18}O in carbonates during contact metamorphism at Maryville, Montana: Implications for isotope systematics in impure dolomitic limestones. Am J Sci 280:890–906

McCrea JM (1950) On the isotopic chemistry of carbonates and a paleotemperature scale. J Chem Phys 18:849–857

Nabelek PI, O'Neil JR, Papike JJ (1983) Vapor phase exsolution as a controlling factor in hydrogen isotope variation in granitic

rocks: The Notch Peak granitic stock, Utah. Earth Planet Sci Lett 66:137–150

Nabelek PI, Hanson GN, Papike JJ, Laul JC (1984a) A melting model for the petrogenesis of an inversely zoned granitic stock, Notch Peak, Utah. (in prep)

Nabelek PI, White CE, Papike JJ (1984b) An inversely zoned granitic stock, Notch Peak, Utah: Mineralogy, petrology, and physical state of the magma. (in prep)

O'Neil JR, Taylor HP Jr (1967) The oxygen isotope and cation exchange chemistry of feldspars. Am Mineral 5:1414–1437

Rice JM (1977) Progressive matamorphism of impure dolomitic limestone in the Marysville aureole, Montana. Am J Sci 277:1–24

Rice JM, Ferry JM (1982) Buffering, infiltration, and the control of intensive variables during metamorphism. In: Ferry JM (ed) Characterization of Metamorphism through Mineral Equilibria, Mineral Soc Am, pp 263–324

Rumble D (1982) Stable isotope fractionation during metamorphic devolatalization reactions. In: Ferry JM (ed) Characterization of Metamorphism through Mineral Equilibria, Mineral Soc Am, pp 327–353

Rumble D, Ferry JM, Hoering TC, Boucot AJ (1982) Fluid flow during metamorphism at the Beaver Brook fossil locality. Am J Sci 283:886–919

Shelton KL (1983) Composition and origin of ore-forming fluids in a carbonate-hosted porphyry copper and skarn deposit: A fluid inclusion and stable isotope study of Mines Gaspé, Quebec. Econ Geol 78:387–421

Shieh YN, Taylor HP Jr (1969) Oxygen and carbon isotope studies of contact metamorphism of carbonate rocks. J Petrol 10:307–331

Shmonov VM, Shmulovich KI (1974) Modal volumes and equation of state of CO_2 at temperatures from 100 to 1000° C and pressures from 2000 to 10000 bars[2]. Doklady Akad. Nauk SSSR 217:206–209

Suzuoki T, Epstein S (1976) Hydrogen isotope fractionation between OH-bearing minerals and water Geochim. Cosmochim. Acta 40:1229–1240

Taylor BE, O'Neil JR (1977) Stable isotope studies of metasomatic Ca–Fe–Al–Si skarns and associated metamorphic and igneous rocks, Osgood Mountains, Nevada. Contrib Mineral Petrol 63:1–49

Taylor HP JR (1974) The application of oxygen and hydrogen isotope studies to problems of hydrothermal alteration and ore deposition. Econ Geol 69:843–883

Taylor HP Jr (1977) Water/rock interaction and the origin of H_2O in granitic batholiths. J Geol Soc Lond 133:509–558

Tracy RJ, Rye DM, Hewitt DA, Schiffries C (1983) Another look at the metamorphism of impure marbles, south-central Connecticut: Isotope petrology. Am J Sci (in press)

Truesdell AH (1974) Oxygen isotope activities and concentrations in aqueous salt solutions at elevated temperatures – consequences for isotope geochemistry. Earth Planet Sci Lett 23:387–396

Valley JW, O'Neil JR (1981) $^{13}C/^{12}C$ exhange between calcite and graphite: a possible thermometer in Grenville marbles. Geochim Cosmochim Acta 45:411–419

Wada H, Suzuki K (1983) Carbon isotopic thermometry calibrated by dolomite calcite solvus temperatures. Geochim Cosmochim Acta 47:697–706

Received October 4, 1983; Accepted January 1, 1984